

SYNTHESIS, MASS SPECTRA, RAMAN AND INFRARED SPECTRA OF THE COMPOUNDS $M(PF_3)_6$ ($M = Cr, Mo, W$)

K. M. LEE and R. E. HESTER

Department of Chemistry, University of York, York (Great Britain)

(Received December 11th, 1972)

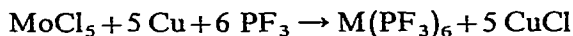
SUMMARY

An improved method of synthesis of hexakis(trifluorophosphine)chromium(0), -molybdenum(0) and -tungsten(0) is described, involving photochemically induced substitution of carbonyl groups from the (trifluorophosphine) tricarbonylmetallates by PF_3 under moderate pressure. A full analysis of the fragmentation patterns in a mass spectrometer is given, and both Raman and infrared data obtained throughout the range $4000-50\text{ cm}^{-1}$ are discussed. Complete vibrational mode assignments are made, and a normal coordinate analysis leading to the determination of force constants and potential energy distributions is presented. The normal mode in which M-P bond stretching is predominant in all cases involves a significant contribution from P-F bond stretching in these molecules.

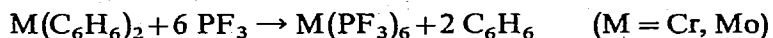
INTRODUCTION

The syntheses and some chemical properties of the hexakis(trifluorophosphine)-metallates of Cr^0 , Mo^0 and W^0 have been described previously by several workers¹⁻⁷. However, the spectroscopy of these structurally interesting compounds has been little studied. No mass spectra or Raman spectra have been reported previously, and the published infrared data refer only to the P-F stretching region.

Previous synthetic routes to these $M(PF_3)_6$ compounds have suffered from disadvantages of low yield and/or extreme experimental conditions. The first syntheses of $M(PF_3)_6$, reported by Kruck and coworkers^{1,2}, involved reduction of the anhydrous metal halides ($MoCl_5$, WCl_6) with copper, which acts as a halogen acceptor, and the simultaneous addition of PF_3 at pressures in the 300 atm range and temperatures around 520 K. The yields, however, were low, the highest recorded being 15% for the reaction:



A further disadvantage is the need for an efficient high-pressure autoclave system. Kruck³⁻⁵ also used a similar technique to induce ligand exchange in suitably coordinated complexes, *viz.* at 600 atm and 570 K,



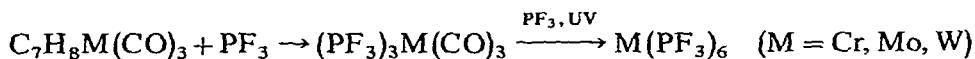
Again, yields no greater than 10% were recorded and features in the 2000 cm^{-1} region of the reported spectra suggested an impure product. Clark and Hoberman⁶ used PF_3 at atmospheric pressure to prepare a mixture of compounds of general formula $\text{Mo}(\text{CO})_{6-n}(\text{PF}_3)_n$, with $n=3$ to 6, from $\text{Mo}(\text{CO})_6$ starting material, under the influence of UV-irradiation. Very small amounts of $\text{Cr}(\text{PF}_3)_6$ were obtained in good yield by Timms⁷ by reaction of Cr vapour, produced from a hot filament, with excess PF_3 in a special stainless steel chamber.

The first part of the present work was to improve on these established synthetic techniques, to devise a procedure resulting in $\text{M}(\text{PF}_3)_6$ products of high purity and in good yield for each of the metals Cr, Mo and W. This serves as a prerequisite for the spectroscopy described in the second part.

EXPERIMENTAL

Syntheses

The general method used involved reaction of cycloheptatrienemetal (Cr, Mo and W) tricarbonyl with PF_3 to produce a mixture of *cis*- and *trans*-(trifluorophosphine)metal tricarbonyl by olefin displacement. This was followed by photochemically induced total substitution of the remaining carbonyls by PF_3 at sub-atmospheric pressure in a sealed Carius tube under UV-irradiation at room temperature (293 K), *viz.*

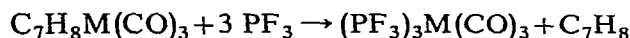


In a typical reaction, 2.5 g of $\text{C}_7\text{H}_8\text{M}(\text{CO})_3$ were placed in a 100 ml thick-walled Carius tube under a dry nitrogen atmosphere provided by a standard glove bag. The tube was transferred to a vacuum line, evacuated, and 4.9 g (5.6 mmol) PF_3 condensed into it at liquid nitrogen temperature (77 K). This quantity of PF_3 was calculated to give 10–12 atm in the sealed tube at room temperature. After sealing under vacuum, the Carius tube was placed in a steel container for 48 h, when the bright red cycloheptatriene complex was transformed into products: a colourless liquid, a colourless crystalline solid, and a brown solid deposited on the tube walls. The excess PF_3 was removed for re-use on the vacuum line by distillation at 178 K (toluene slush), and then distillation from the tube at 273 K through a series of traps at 253 K (ice-salt), 237 K (dichloroethylene slush), and 178 K separated the $(\text{PF}_3)_3\text{M}(\text{CO})_3$ (passed the 253 K trap, but stopped in the 237 K trap) and cycloheptatriene (stopped in the 253 K trap) products.

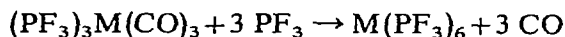
The $(\text{PF}_3)_3\text{M}(\text{CO})_3$ was next condensed into an irradiation flask at liquid nitrogen temperature. This spherical, one litre flask had a 10 cm long, 2 cm i.d. fused quartz extension tube of 1 mm wall thickness which allowed useful transmission of radiation to a short wavelength limit of 200 nm. 20 ml n-hexane and PF_3 to a pressure of 500 mmHg were transferred to the flask on the vacuum line. The quartz extension tube was then irradiated with a 400 watt medium pressure mercury arc lamp (Hanau model Q400), collected with a large spherical reflector and focussed onto the sample with quartz lenses, for several periods each of 16 h. Between each period the contents of the irradiation flask were condensed into the extension tube at 77 K, the CO released by the reaction was pumped away and more PF_3 introduced to restore its partial

pressure to 500 mmHg. Completion of the reaction was signalled by the cessation of CO production. Finally, with the extension tube at 263 K (ice-salt), the n-hexane and excess PF_3 were distilled away from the $M(\text{PF}_3)_6$ product. This product was purified by sublimation at room temperature (293 K) and 10^{-3} mmHg, and was stored under dry N_2 .

For the reaction:



the yields were: Cr, 53; Mo, 49; W, 58 %, based on $\text{C}_7\text{H}_8\text{M}(\text{CO})_3$ starting material. For the following procedure:



the yields were quantitative. The $\text{C}_7\text{H}_8\text{M}(\text{CO})_3$ starting materials were prepared by the method of Bennett, Pratt and Wilkinson⁸ for $M = \text{Cr}$ and Mo , and by King's⁹ method for $M = \text{W}$, since in this latter case the metal hexacarbonyl did not react with C_7H_8 under the conditions prescribed for Cr and Mo. PF_3 was prepared from PCl_3 by reaction with ZnF_2 according to the method of Williams¹⁰. Reagent grade chemicals were used throughout, the $\text{M}(\text{CO})_6$ compounds being purified by sublimation before use.

In moist air the $\text{M}(\text{PF}_3)_6$ compounds turned a pale blue colour after only 24 h, and therefore all manipulations of these materials were performed under a dry nitrogen atmosphere. Some physical properties of the compounds are listed in Table 1, the melting points and decomposition temperatures being determined with the compounds in sealed capillary tubes, with heating continued until decomposition yielded a black residue and a metallic mirror was deposited on the walls of the tube. The wide liquid range of these compounds prior to decomposition was to prove extremely useful in obtaining Raman spectra of the liquid phases.

Elemental analyses were performed by the Bernhardt Ltd. Microanalytical Laboratory for both P and F and were in all cases in excellent agreement with theory. Mass spectra, presented in the following section, provided further confirmation of the product identities.

Spectroscopy

Mass spectra were obtained using a standard A.E.I. MS-12 mass spectrometer,

TABLE 1

SOME PHYSICAL PROPERTIES OF THE COMPOUNDS $\text{M}(\text{PF}_3)_6$ ($M = \text{Cr, Mo, W}$)

Compound	Melting point (K)	Decomposition Temp. (K)	Vapour Pressure at 295 K/mmHg)
$\text{Cr}(\text{PF}_3)_6$	469 (Lit. ¹ 466)	Above 573	2
$\text{Mo}(\text{PF}_3)_6$	473 (Lit. ¹ 469)	Above 548	1.5
$\text{W}(\text{PF}_3)_6$	487 (Lit. ¹ 487)	Above 578	1.5

operating with 70 eV electron energy.

Infrared spectra were obtained using a Perkin-Elmer model 621 spectrometer for the region $4000-200\text{ cm}^{-1}$, and a Grubb-Parsons Cube Interferometer, equipped with a 6.25 micron thick beam splitter, for the region $400-30\text{ cm}^{-1}$. A 100 mm path length cell fitted with CsI windows was used for vapour phase spectra. The solids were run as nujol and hexachlorobutadiene mulls held between CsI plates for the middle infrared, and as vaseline mulls between polyethylene plates for the far infrared. Concentrations as high as 70% w/w were required to obtain reasonable intensity in the bands attributed to M-P stretching (at ca. 200 cm^{-1} ; see latter discussion).

TABLE 2

MASS SPECTRA OF THE COMPOUNDS $\text{Cr}(\text{PF}_3)_6$, $\text{Mo}(\text{PF}_3)_6$ AND $\text{W}(\text{PF}_3)_6$

	Ion	<i>m/e</i> ; Relative intensities		
		Cr	Mo	W
A	$\text{M}(\text{PF}_3)_6^+$	580; 39.4	625; 73.5	717; 61.2
B	$\text{M}(\text{PF}_3)_5(\text{PF}_2)^+$	561; 21.2	606; 16.9	693; 10.6
C	$\text{M}(\text{PF}_3)_5(\text{PF})^+$			674; 19.6
D	$\text{M}(\text{PF}_3)_5(\text{F})^+$			643; 5.1
E	$\text{M}(\text{PF}_3)_5^+$	492; 24.3	537; 9.7	624; 11.2
F	$\text{M}(\text{PF}_3)_4(\text{PF}_2)^+$		518; 38.6	
G	$\text{M}(\text{PF}_3)_4(\text{F})^+$	423; ca. 0.5		555; 9.5
H	$\text{M}(\text{PF}_3)_4^+$	404; 60.7	449; 26.5	536; 28.5
I	$\text{M}(\text{PF}_3)_3(\text{PF}_2)^+$		430; 22.9	517; 15.9
J	$\text{M}(\text{PF}_3)_3(\text{F})^+$	335; 18.2	380; 5.0	467; 15.4
K	$\text{M}(\text{PF}_3)_3^+$	316; 19.4	361; 48.2	448; 50.4
L	$\text{M}(\text{PF}_3)_2(\text{PF}_2)^+$	297; 1.2	342; 22.9	429; 10.2
M	$\text{M}(\text{PF}_3)_2(\text{PF})^+$			410; 5.0
N	$\text{M}(\text{PF}_3)_2(\text{F})^+$	247; ca. 0.4	292; 4.8	399; 9.4
O	$\text{M}(\text{PF}_3)_2^+$	228; 55.7	273; 68.7	360; 67.6
P	$\text{M}(\text{PF}_3)(\text{PF}_2)^+$	209; 19.7	254; 13.1	341; 14.0
Q	$\text{M}(\text{PF}_3)(\text{PF})^+$	190; ca. 0.2	235; 4.6	322; 27.6
R	$\text{M}(\text{PF}_3)(\text{F})^+$	159; 15.1	204; 15.7	291; 10.2
S	$\text{M}(\text{PF}_3)^+$	140; 100	185; 100	272; 100
T	$\text{M}(\text{PF}_2)^+$	121; 7.0	166; 19.3	253; 19.4
U	MF_3^+		154; 2.0	
V	$\text{M}(\text{PF})^+$	102; 3.3	147; 9.6	234; 6.3
W	MF_2^+		135; 1.0	
X	MP^+	83; 3.0		215; 10.0
Y	MF^+	71; 60.5	116; 27.7	203; 4.2
Z	M^+	51→54	91→98	182→186
	PF_3^+	88; 321	88; 351	88; 561
	PF_2^+	69; 479	69; 522	69; 324
	PF^+	50; ^{50}Cr	50; 280	50; 492
		coincident		
	P^+	31; 851	31; 16	31; 91
<i>Metastable peaks:</i>		<i>m/e</i>	<i>m/e</i>	
		417 (A→C)	442 (B→F)	
		332 (E→H)		
		86 (O→S)		

Solutions in *n*-hexane (spectro grade) were run in a standard liquid cell, with a 50 micron path length and CsI windows. The standard Grubb-Parsons variable temperature cell was used for samples run at 77 K in the far infrared region.

Raman spectra were obtained principally with an instrument based on a Hilger and Watts D330/331 double monochromator coupled with a Brookdeal phase sensitive detection system, using a Spectra-Physics model 125 He/Ne laser at 632.8 nm for excitation. Solid samples were held in a slotted stainless steel block or in pyrex glass capillary tubes. A small furnace¹¹ was used to melt the compounds in sealed pyrex glass tubes for liquid phase Raman studies. A Coderg PH-1 spectrometer, with an O.I.P. He/Ne laser, was used for the low frequency region 150–40 cm^{-1} where its superior stray light rejection characteristics were advantageous. Bond polarization data were determined by rotation of the plane of polarization of the incident light with a half-wave plate.

All sample cells were filled in a dry nitrogen atmosphere within a glove box. Frequencies are reported accurate to $\pm 3 \text{ cm}^{-1}$.

SPECTROSCOPIC RESULTS

Mass spectra obtained from the purified compounds $\text{Cr}(\text{PF}_3)_6$, $\text{Mo}(\text{PF}_3)_6$ and $\text{W}(\text{PF}_3)_6$ are reported in Table 2, together with the species assigned as responsible for each of the peaks observed. In each case the spectra were more complicated than is suggested by the data given in Table 2 due to the natural occurrence of the metals Cr, Mo and W as mixtures of isotopes. However the characteristic isotope patterns served as a useful aid to assignments of metal-containing fragments. Relative intensities are reported on the basis of peak heights associated with the most abundant isotopes: ^{52}Cr (83.46% natural abundance), ^{98}Mo (23.8%) and ^{184}W (30.7%). Metastable species were characterised by very weak broad peaks and provide excellent corroboratory evidence regarding the fragmentation of species assigned in Table 2. In each case the processes correspond to the elimination of PF_3 or F.

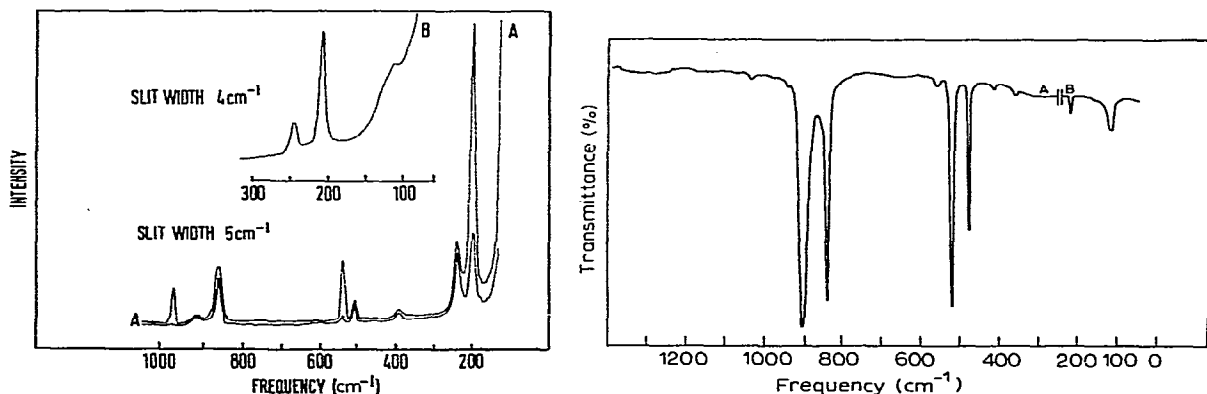


Fig. 1. Raman spectra of $\text{Cr}(\text{PF}_3)_6$: A, molten sample showing band polarization characteristics; B, crystalline solid sample in low frequency region.

Fig. 2. Infrared spectra of $\text{Cr}(\text{PF}_3)_6$: A, vapour phase spectrum (10 cm path length, 2 mmHg vapour pressure); B, solid mull in vaseline. Far infrared region.

TABLE 3

INFRARED SPECTRA OF $C_1(PF_3)_6$, $M_0(PF_3)_6$, $W(PF_3)_6$ IN THE SOLID, LIQUID, AND VAPOUR PHASES^{a,b}

$C_1(PF_3)_6$			$M_0(PF_3)_6$			$W(PF_3)_6$			Assignments
Lit. data	Vapour	Liquid Solid Intensity	Lit. data	Vapour	Liquid Solid Intensity	Lit. data	Vapour	Liquid Solid Intensity	
		1800 vvw			1800 vvw			1725 vvw	$\nu_1 + \nu_{14}$ $\nu_5 + \nu_{14}$
		1715 vvw			1720 vvw				OR $\nu_{13} + \nu_{20}$
		1690 vvw			1690 vvw			1695 vvw	$\nu_{14} + \nu_{20}$
	1045	1035 vw(br)		1045	1045 vw(br)		1058	1045 vw	$\nu_3 + \nu_{14}$
	948	945 vw		950	950 vw		955	950 vw	$\nu_{14} + \nu_{22}$
916 ^c	916	905 vs(br)		912	903 vs(br)	914 ^c	913	900 vs(br)	$\nu_{13}T_{1u}$
			902 ^d						
851 ^c	851	842 s(sp)	853 ^c 845 ^d	850	845 s(sp)	825 ^c	851	843 s(sp)	$\nu_{14}T_{1u}$
	568	565 w(sh)		529	530 w(sh)		565	560 w(sh)	$\nu_3 + \nu_{19}$
	529	524 s(br)		498	480 s		500	492 s(br)	$\nu_{15}T_{1u}$
	485	480 s(sp)		429	425 s(sp)		412	405 m	$\nu_{16}T_{1u}$
		415 418 w		405	405 w			395 w(sh)	$\nu_3 + \nu_{17}$
	365	365 w		330	330 w			297 w(sp)	OR $\nu_{15} - \nu_{22}$
		217 vw		209	209 w			215 w	$\nu_{19}T_{1u}$
		116 m		90	90 m			88 m	$\nu_{17}T_{1u}$ $\nu_{18}T_{1u}$

^a All frequencies in cm^{-1} ; w = weak; m = medium; s = strong; v = very; (br) = broad; (sp) = sharp; (sh) = shoulder. ^b The column heading "Lit. data" refers to the literature data for the vapour and hexane solution phases. ^c See Ref. 1. ^d See Ref. 6.

The compounds were further characterised by the following UV absorption bands, these being obtained from cyclohexane solutions:

$\text{Cr}(\text{PF}_3)_6$: λ_{max} at 216 nm ($\log \epsilon$, 4.04) with a shoulder at 285 nm (2.64);

$\text{Mo}(\text{PF}_3)_6$: λ_{max} at 208.5 nm (3.99), and 234 nm (4.16) with a shoulder at 258 nm (3.36);

$\text{W}(\text{PF}_3)_6$: λ_{max} at 212 nm (4.30), and 232 nm (4.40) with a shoulder at 256 nm (3.70).

Raman and infrared spectra of the compounds $\text{Cr}(\text{PF}_3)_6$, $\text{Mo}(\text{PF}_3)_6$ and $\text{W}(\text{PF}_3)_6$ are shown in Figs. 1 to 6. In each case the full Raman spectra are shown for the pure compounds run as liquids, and the low frequency regions from spectra of crystalline solids also are shown. Infrared spectra are shown for vapour phase samples in the middle-infrared region, and for vaseline mulls of solid samples in the far-infrared. Infrared frequencies are listed in Table 3 and Raman frequencies in Table 4.

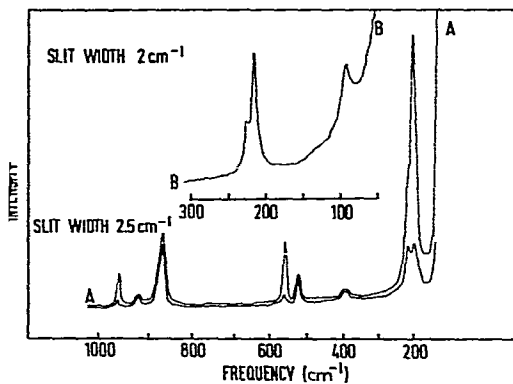


Fig. 3. Raman spectra of $\text{Mo}(\text{PF}_3)_6$: A, molten sample showing band polarization characteristics; B, crystalline solid sample in low frequency region.

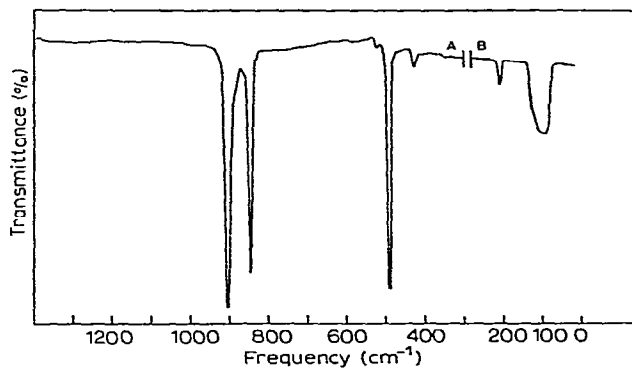


Fig. 4. Infrared spectra of $\text{Mo}(\text{PF}_3)_6$: A, vapour phase spectrum (10 cm path length, 2 mmHg vapour pressure); B, solid mull in vaseline. Far infrared region.

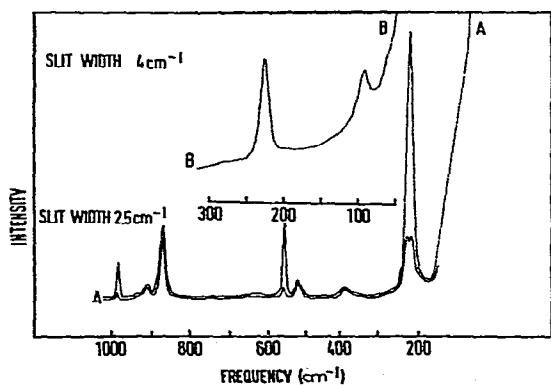


Fig. 5. Raman spectra of $\text{W}(\text{PF}_3)_6$: A, molten sample showing band polarization characteristics; B, crystalline solid sample in low frequency region.

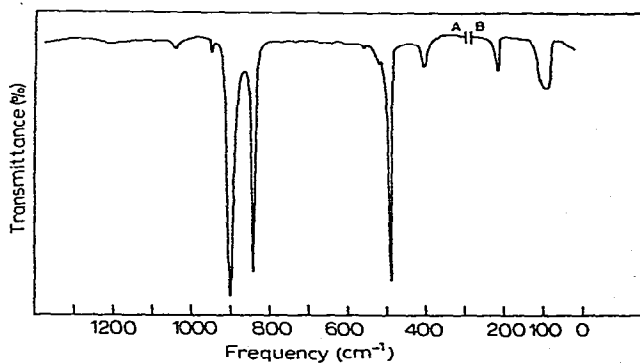


Fig. 6. Infrared spectra of $\text{W}(\text{PF}_3)_6$: A, vapour phase spectrum (10 cm path length, 2 mmHg vapour pressure); B, solid mull in vaseline. Far infrared region.

TABLE 4

RAMAN SPECTRA (CM^{-1}) OF $\text{Cr}(\text{PF}_3)_6$, $\text{Mo}(\text{PF}_3)_6$, AND $\text{W}(\text{PF}_3)_6$ IN THE SOLID AND LIQUID PHASE^a

$\text{Cr}(\text{PF}_3)_6$			$\text{Mo}(\text{PF}_3)_6$			$\text{W}(\text{PF}_3)_6$			Assignments
Solid	Liquid	Polarization and intensities	Solid	Liquid	Polarization and intensities	Solid	Liquid	Polarization and intensities	
974	968	mw, pol	967	958	mw, pol	972	971	mw, pol	$\nu_1 A_{1g}$
908	908	w, dep	901	896	w, dep	901	895	w, dep	$\nu_5 E_g$
859	852	m, dep	861	852	m, dep	861	860	m, dep	$\nu_{20} T_{2g}$
549	544	m, pol	549	540	m, pol	551	554	m, pol	$\nu_2 A_{1g}$
519	509	m, dep	514	507	mw, dep	516	519	mw, dep	$\nu_6 E_g$
396	398	w(br), dep	387	382	w(br), dep	384	382	w(br), dep	$\nu_{21} T_{2g}$
238	242	m, dep	224	215	m, dep		215	m, dep	$\nu_7 E_g$
209	200	vvs, pol	214	204	vvs, pol	221	224	vvs, pol	$\nu_3 A_{1g}$
111		m, dep ?	86		m, dep ?	84		m, dep ?	$\nu_{22} T_{2g}$

^a Pol=polarized; dep=depolarized; ?=state of polarization uncertain.

DISCUSSION

Treatment of the vibrational modes of the molecules $\text{M}(\text{PF}_3)_6$ is greatly simplified by the assumption of free rotation about the M-P bonds. The method developed by Crawford and Wilson¹² may be applied to this situation, treating the molecule $\text{M}(\text{PF}_3)_6$ as an MP_6 octahedral framework with a symmetrical PF_3 to be attached at each P atom. However, the further approximation suggested by Cotton¹³ for $\text{M}(\text{XY}_3)_6$ species of neglecting interactions of the several XY_3 ligands with one another is not justified by the appearance of the spectra as will be apparent from the following analysis.

The vibrational modes of the octahedral framework (symmetry O_h) are of the species $A_{1g} + E_g + 2T_{1u} + T_{2g} + T_{2u}$. The purely internal modes of a M-PF_3 group of C_{3v} local symmetry are of the species $2A_1 + 3E$. These ligand modes may be combined in the overall reduced O_h symmetry of the $\text{M}(\text{PF}_3)_6$ molecule by the standard method of vector combinations, resulting in an overall representation of the total vibrational motion as follows:

$$\Gamma_{\text{vib}} = 3A_{1g} + A_{1u} + 3E_g + E_u + 4T_{1g} + 7T_{1u} + 4T_{2g} + 4T_{2u}$$

Of these 27 fundamentals, 10 will be Raman active ($3A_{1g} + 3E_g + 4T_{2g}$), 7 will be infrared active ($7T_{1u}$), and the remaining 10 ($A_{1u} + E_u + 4T_{1g} + 4T_{2u}$) will be inactive in both Raman and infrared spectra. Approximate descriptions of all 27 modes of vibration, as P-F stretching, M-P deformation, etc., are summarized in Table 5.

The assignments of active fundamentals given in Tables 3 and 4 have been derived primarily by comparison with related molecular spectra. For example, the P-F symmetric stretching mode of the free PF_3 molecule lies in the 900 cm^{-1} region¹⁴, and the symmetric P-F deformation at ca. 500 cm^{-1} . The symmetric M-P stretching modes of metal complexes commonly have been reported¹⁵ to occur in the 200 cm^{-1} region. On the basis, the three strongly polarized Raman bands are unambiguously assigned as in Table 4.

TABLE 5

NATURE, SYMMETRY SPECIES AND ACTIVITY OF THE NORMAL VIBRATIONS^a OF THE $M(\text{PF}_3)_6$ DERIVATIVES FOR THE POINT GROUP O_h

Type	No.	P-F str (ν_1)	P-F str (ν_2)	P-F def (ν_3)	P-F def (ν_4)	M-P str	M-P def	PF_3 twist	PF_3 rock	Activity
A_{1g}	3	ν_1		ν_2		ν_3				Raman polarized
A_{1u}	1							ν_4		Inactive
A_{2g}	0									Inactive
A_{2u}	0									Inactive
E_g	3	ν_5		ν_6		ν_7				Raman depolarized
E_u	1							ν_8		Inactive
T_{1g}	4		ν_9		ν_{10}			ν_{11}	ν_{12}	Inactive
T_{1u}	7	ν_{13}	ν_{14}	ν_{15}	ν_{16}	ν_{17}	ν_{18}		ν_{19}	Infrared active
T_{2g}	4		ν_{20}		ν_{21}		ν_{22}		ν_{23}	Raman depolarized
T_{2u}	4		ν_{24}		ν_{25}		ν_{26}		ν_{27}	Inactive

^a str = Stretch; def = deformation. Symbols in parentheses indicate simple PF_3 modes.

The spectral region $800\text{--}1000\text{ cm}^{-1}$ may be designated the P-F stretching region. In addition to the $\nu_1(A_{1g})$ band, there also are observed two Raman depolarized bands in this region. For $\text{Cr}(\text{PF}_3)_6$ these are at 859 and 908 cm^{-1} . Although their assignment to degenerate P-F asymmetric stretching modes seems clear, the specific assignments of 908 cm^{-1} to $\nu_5(E_g)$ and 859 cm^{-1} to $\nu_{20}(T_{2g})$ depended on a full normal coordinate analysis, details of which are presented later. Similarly, the assignments of strong infrared bands in the $\text{Cr}(\text{PF}_3)_6$ spectrum at 885 to $\nu_{13}(T_{1u})$ and 835 cm^{-1} to $\nu_{14}(T_{1u})$ are made by comparison with simple PF_3 modes and for consistency in the normal coordinate analysis.

In the P-F deformation region, $350\text{--}600\text{ cm}^{-1}$, besides the $\nu_2(A_{1g})$ band two further Raman bands were observed in the $\text{Cr}(\text{PF}_3)_6$ spectrum at 519 and 396 cm^{-1} . The comparison with the PF_3 result¹⁴ suggests that these are $\nu_6(E_g)$ and $\nu_{21}(T_{2g})$, respectively. Five infrared bands occur in this P-F deformation region. The two most intense bands are assigned to fundamentals $\nu_{15}(T_{1u})$ and $\nu_{16}(T_{1u})$, while the very weak bands at 563 and 418 cm^{-1} appear to arise from combinations of lower frequency modes (see Table 3). The fifth infrared band, also very weak, is at 366 cm^{-1} for $\text{Cr}(\text{PF}_3)_6$ and is assigned to the $\nu_{19}(T_{1u})$ PF_3 rocking mode by analogy with the analysis of $M(\text{PF}_3)_4$ spectra by Woodward and coworkers^{16,17}.

The frequency region below 300 cm^{-1} contains bands characterising M-P stretching and P-M-P deformation modes. Apart from the intense and polarized Raman band [at 200 cm^{-1} for $\text{Cr}(\text{PF}_3)_6$] which is unambiguously assigned to the $\nu_3(A_{1g})$ M-P stretching mode, there are two medium intensity depolarized Raman bands to be assigned [at 238 and 111 cm^{-1} for $\text{Cr}(\text{PF}_3)_6$]. The former is largely obscured by the much more intense ν_3 band for the Mo and W compounds, but selective attenuation of ν_3 by changing from parallel to perpendicularly polarized excitation clearly reveals its presence (see Figs. 1, 3, and 5). Its proximity to ν_2 suggests its assignment to $\nu_7(E_g)$, the M-P asymmetric stretch, leaving the lower frequency Raman band as $\nu_{22}(T_{2g})$, a P-M-P deformation mode. The infrared bands in this region follow similarly, the higher frequency one [at 217 cm^{-1} for $\text{Cr}(\text{PF}_3)_6$] being

TABLE 6

FORCE CONSTANTS FOR THE COMPOUNDS $M(\text{PF}_3)_6$ ($M = \text{Cr}, \text{Mo}$ AND W)

Compound	Force constants ($\text{N} \cdot \text{m}^{-1}$)		
	$K(\text{P-F})$	$K(\text{F-P-F})$	$K(\text{M-P})$
$\text{Cr}(\text{PF}_3)_6$	780	100	290
$\text{Mo}(\text{PF}_3)_6$	780	100	320
$\text{W}(\text{PF}_3)_6$	770	100	390

TABLE 7

VIBRATIONAL ANALYSIS RESULTS FOR $M(\text{PF}_3)_6$ DERIVATIVES

Mode of vibration	Frequency (cm^{-1})		Potential energy distribution					
	Obs.	Calcd.	$\nu(\text{P-F})$	$\delta(\text{PF}_3)$	$\nu(\text{M-P})$	$\delta(\text{MP}_2)$	$\delta(\text{MPF})$	
A. $\text{Cr}(\text{PF}_3)_6$								
A_{1g}	ν_1	974	973	0.86	0.07	0.07	0	0
	ν_2	549	545	0.13	0.56	0.31	0	0
	ν_3	209	207	0.01	0.39	0.60	0	0
E_g	ν_5	908	972	0.88	0.06	0.06	0	0
	ν_6	519	541	0.13	0.58	0.30	0	0
	ν_7	238	205	0.01	0.39	0.60	0	0
T_{1u}	ν_{13}	885	1155	0.92	0.03	0	0.02	0.02
	ν_{14}	835	971	0.85	0.06	0.06	0	0
	ν_{15}	517	636	0.10	0.11	0.55	0.15	0.08
	ν_{16}	480	453	0.05	0.64	0	0.19	0.13
	ν_{17}	217	237	0	0.14	0.29	0	0.60
	ν_{18}	116	125	0	0.07	0.15	0.61	0.17
	ν_{19}	366	387	0	0.95	0.02	0	0.02
T_{2g}	ν_{20}	859	1163	0.92	0.03	0	0.03	0.02
	ν_{21}	396	404	0.06	0.83	0	0.10	0.01
	ν_{22}	111	126	0	0.06	0	0.70	0.24
	ν_{23}	?	279	0.02	0.08	0	0.17	0.73
B. $\text{Mo}(\text{PF}_3)_6$								
A_{1g}	ν_1	967	976	0.86	0.07	0.07	0	0
	ν_2	549	552	0.14	0.53	0.33	0	0
	ν_3	214	213	0.02	0.42	0.58	0	0
E_g	ν_5	901	955	0.87	0.07	0.07	0	0
	ν_6	514	549	0.14	0.54	0.32	0	0
	ν_7	224	210	0	0.42	0.58	0	0

(Continued)

TABLE 7 (continued)

Mode of vibration	Frequency (cm^{-1})		Potential energy distribution					
	Obs.	Calcd.	$\nu(\text{P-F})$	$\delta(\text{PF}_3)$	$\nu(\text{M-P})$	$\delta(\text{MP}_2)$	$\delta(\text{MPF})$	
T_{1u}	ν_{13}	885	1152	0.94	0.03	0	0.02	0.02
	ν_{14}	835	971	0.86	0.06	0.08	0	0
	ν_{15}	480	575	0.12	0.31	0.51	0.04	0.02
	ν_{16}	425	408	0.05	0.64	0	0.18	0.10
	ν_{17}	209	238	0	0.16	0.29	0	0.54
	ν_{18}	90	119	0	0.05	0.10	0.68	0.16
	ν_{19}	330	373	0	0.70	0.09	0.07	0.15
	ν_{20}	861	1159	0.92	0.03	0	0.03	0.01
	ν_{21}	387	401	0.06	0.85	0	0.08	0
T_{2g}	ν_{22}	86	122	0	0.05	0	0.74	0.21
	ν_{23}	?	273	0.02	0.06	0	0.16	0.77
<i>C. W(PF₃)₆</i>								
A_{1g}	ν_1	972	975	0.85	0.08	0.07	0	0
	ν_2	551	554	0.18	0.52	0.30	0	0
	ν_3	221	223	0.01	0.45	0.54		
E_g	ν_5	901	974	0.86	0.08	0.06	0	0
	ν_6	516	547	0.14	0.56	0.30	0	0
	ν_7	215	212	0	0.41	0.59	0	0
T_{1u}	ν_{13}	887	1153	0.93	0.02	0.02	0	0.02
	ν_{14}	839	974	0.88	0.08	0.04	0	0
	ν_{15}	484	580	0.14	0.35	0.49	0.02	0
	ν_{16}	404	388	0.06	0.60	0	0.20	0.12
	ν_{17}	216	236	0	0.16	0.31	0	0.51
	ν_{18}	88	114	0	0.02	0.14	0.72	0.12
	ν_{19}	297	360	0	0.61	0.12	0.06	0.21
	ν_{20}	861	1160	0.93	0.03	0	0.03	0.01
	ν_{21}	384	396	0.05	0.86	0	0.07	0.02
	ν_{22}	84	118	0	0.01	0	0.77	0.22
ν_{23}	?	271	0.04	0.06	0	0.12	0.76	

$\nu_{17}(T_{1u})$, the M-P asymmetric stretch, and the lower (116 cm^{-1}) being $\nu_{18}(T_{1u})$, a P-M-P asymmetric deformation. All the remaining bands listed in Table 3 are very weak and may satisfactorily be assigned to combination tones as indicated in the Table.

Normal coordinate analysis

The determination of force constants and distribution of potential energy among the vibrational modes for the molecules $M(\text{PF}_3)_6$ was based on a computer program, "INTVIBANAL", devised by Gilson¹⁸. This program employed the standard Wilson FG-matrix methods¹⁹ and was available on a library file at the S.R.C. Atlas Computing Centre in Didcot. The primary purpose of the analysis was to obtain a confirmation of the band assignments and for this it was considered acceptable to use an initial set of force constants and molecular geometry parameters

“borrowed” from similar molecules¹⁷. The calculation then “refined” these values to provide the best fit achievable with the experimental frequencies, based on a simple valence force field¹⁹. In the absence of X-ray crystallographic data on the molecules a more elaborate treatment was considered unjustified.

Some results of these calculations are quoted in Tables 6 and 7. The force constants were refined primarily to produce frequencies in agreement with the experimental values determined for the A_{1g} modes of each of the compounds, these being the modes assigned empirically with maximum confidence. From the data given in Table 7 it is apparent that the agreement achieved between calculated and experimental frequencies was often poor for modes of lower symmetry. However, in spite of this the calculated ordering of modes on the frequency scale parallels that determined experimentally, so that some additional confidence may be placed on the band assignments made.

In so far as approximate force constants of this type may be taken as a guide to the nature of changes in bonding in this series of transition metal trifluorophosphine compounds it is interesting to note that the P–F stretching and F–P–F angle deformation mode force constants are essentially constant throughout the series. However, the metal–ligand stretching force constant, $F(M-P)$, increases significantly from Cr to Mo to W. This behaviour is closely similar to that reported¹⁵ for the series $Ni(PF_3)_4$, $Pd(PF_3)_4$ and $Pt(PF_3)_4$, indicating a general “stiffening” of the M–P bonds on moving from a first to a third row transition metal. Metal–phosphorus π -bonding seems unlikely to account for this trend, since the $3d_\pi$ -acceptor orbitals on phosphorus are expected to interact less effectively with $5d_\pi$ -donor orbitals than with $3d_\pi$ -donors, so that we might tentatively suggest increased σ -bond strength down the series to account for these results. Discussion from the experimental band frequency results as to the nature of changes in the metal–ligand bonding are likely to be less fruitful due to the complex character of the modes involved. For example, the data of Table 8 show the mode $\nu_3(A_{1g})$ to involve a mixture of 60% Cr–P stretching, 39% F–P–F angle deformation and 1% P–F stretching for $Cr(PF_3)_6$, this changing to 54% W–P stretching, 45% F–P–F deformation and 1% P–F stretching for $W(PF_3)_6$. It clearly is difficult to draw conclusions about the nature of the M–P bonding from these unprocessed frequency data.

ACKNOWLEDGEMENTS

We thank Dr. Alan Creighton of the University of Kent for spectra from his Coderg PH-1 Raman spectrometer, and the S.R.C. for support for one of us (KML).

REFERENCES

- 1 Th. Kruck and A. Prasch, *Angew. Chem., Int. Ed. Engl.*, 6 (1967) 56.
- 2 Th. Kruck and W. Lang, *Angew. Chem., Int. Ed. Engl.*, 4 (1965) 148.
- 3 Th. Kruck, *Z. Naturforsch. B*, 19 (1964) 165.
- 4 Th. Kruck, *Chem. Ber.*, 97 (1964) 2018.
- 5 Th. Kruck and A. Prasch, *Z. Naturforsch. B*, 19 (1964) 669.
- 6 R. J. Clark and P. I. Hoberman, *J. Inorg. Chem.*, 4 (1965) 1771.
- 7 P. L. Timms, *J. Chem. Soc. D.*, (1969) 1033.

- 8 M. A. Bennet, L. Pratt and G. Wilkinson, *J. Chem. Soc.*, (1961) 2037.
- 9 R. B. King (Ed.), *Organometallic Syntheses*, Academic Press, N. Y., 1965.
- 10 A. A. Williams, *Inorg. Syn.*, 8 (1967) 95.
- 11 J. H. R. Clarke and R. E. Hester, *J. Chem. Phys.*, 50 (1969) 3106.
- 12 B. L. Crawford and E. B. Wilson, *J. Chem. Phys.*, 9 (1941) 323.
- 13 F. A. Cotton in *Modern Coordination Chemistry*, Interscience, New York, 1960.
- 14 M. K. Wilson and S. R. Polo, *J. Chem. Phys.*, 20 (1952) 1716.
- 15 D. M. Adams, *Metal-ligand and Related Vibrations*, Arnold, London, 1967.
- 16 L. A. Woodward and J. R. Hall, *Spectrochim. Acta*, 16 (1960) 654.
- 17 H. G. M. Edwards and L. A. Woodward, *Spectrochim. Acta A*, 26 (1970) 897.
- 18 T. R. Gilson, *Intvibanal*, Department of Chemistry, University of Southampton, 1969.
- 19 E. B. Wilson, Jr., J. C. Decius and P. C. Cross, *Molecular Vibrations, The Theory of Infrared and Raman Vibrational Spectra*, McGraw-Hill, New York, 1955.